

Supplementary Information

Preferential population of Al atom at the T4 site of ZSM-35 for the carbonylation of dimethyl ether

Zhiping Xiong^{a,c,†}, Guodong Qi^{b,†}, Luyi Bai^a, Ensheng Zhan^{a,*}, Yueying Chu^b, Jun Xu^{b,*}, Na Ta^a,
Aijing Hao^{a,c}, Feng Deng^b, Wenjie Shen^a

^a State Key Laboratory of Catalysis, Dalian Institute of Chemical Physics, Chinese Academy of Sciences, Dalian, China.

^b National Centre for Magnetic Resonance in Wuhan, State Key Laboratory of Magnetic Resonance and Atomic and Molecular Physics, Innovation Academy for Precision Measurement Science and Technology, Chinese Academy of Sciences, Wuhan, China.

^c University of Chinese Academy of Sciences, Beijing, China.

[†] These authors contributed equally to the work

* To whom corresponds should be addressed.

E-mail: eszhan@dicp.ac.cn; xujun@wipm.ac.cn

Materials preparation

The ZSM-35 zeolite was synthesized by a hydrothermal method. In a typical procedure, certain amounts of NaOH (96%), NaAlO₂ (96%), SiO₂ colloid, 1,4-dioxane (Diox) and water were mixed at a gel composition of 1.9 NaOH : Al₂O₃ : 21.4 SiO₂ : 427.7 H₂O : 21.9 SDA. The transparent gel was stirred at 323 K for 3 h and transferred to a Teflon-lined stainless-steel autoclave. The mixture was treated at 423 K for 5 days under tumbling conditions. After cooling down to room temperature, the solid product was collected by filtration, washed with water, dried at 383 K overnight and calcined at 823 K in air for 10 h, yielding the Na-form FER. It was then ion-exchanged with a 1.0 M NH₄NO₃ aqueous solution at 353 K for 6 h, and this procedure was repeated for three times for achieving a full ion-exchange. The precipitate was dried at 383 K overnight and calcined at 813 K for 5 h in a flowing 20 % O₂/N₂ mixture, yielding the H-form FER, labelled as ZSM-35-Diox.

A commercial sample (Zeolyst, CP 914C, NH₄-FER) was used for comparative study. It was directly calcined at 813 K for 5 h in a flowing 20% O₂/N₂ mixture, and the H-form sample was named as Zeolyst.

Characterization

Powder X-ray diffraction (XRD) patterns were recorded on a D/MAX 2500/PC diffractometer (Rigaku), using a Cu Ka ($\lambda = 0.154$ nm) radiation source that was operated at 40 kV and 200 mA. Field-emission scanning electron microscopy (FESEM) images were taken on a Philips FEI Quanta 200F microscope operated at 20 kV. Transmission electron microscopy (TEM) images were acquired over a JEM-F200 microscope at 200 kV.

N₂ adsorption-desorption isotherms were recorded on a Micromeritics ASAP-2020 adsorption instrument at 77 K; the sample was outgassed at 573 K for 5 h prior to the measurement. The total surface area was obtained from the BET (Brunauer-Emmet-Teller) equation from the adsorption isotherms at P/P_0 between 0.005 and 0.05, and the total pore volume was calculated from the adsorption isotherms at $P/P_0 = 0.99$. The micropore volume was calculated using the t-plot method.

Elemental analysis of Si and Al was performed on a Plasma-Spec-II-type ICP-AES spectrometer.

Temperature-programmed desorption of ammonia (NH₃-TPD) was conducted with a U-

shaped quartz tube reactor. The sample (100 mg) was heated to 773 K at a rate of 5 K/min and kept at this temperature for 1 h under He flow (30 mL/min). After cooling down to 473 K, the sample was exposed to a 10% NH₃/He mixture (30 mL/min) for 30 min. The physically adsorbed ammonia was removed by consecutively purging the sample at 473 K with He for 1 h, a 0.6% H₂O/He mixture for 1 h and again He for 1 h.¹ Desorption of ammonia was then performed by heating the sample to 923 K at a rate of 10 K/min under He flow (30 mL/min), and the amount of NH₃ desorbed was monitored by a thermal conductivity detector.

Py-IR spectra were recorded over a Bruker Tensor 27 spectrometer with a resolution of 4 cm⁻¹. 15 mg sample was pressed into a self-supporting wafer (R = 0.65 cm) and loaded into an IR cell. The sample was evacuated to 2 × 10⁻² Pa at 673 K for 1 h to remove the physically adsorbed water. After cooling down to room temperature, the background spectrum was recorded. Py adsorption was done at 573 K for 10 min, and the sample was evacuated for 1 h to eliminate the physically adsorbed pyridine. The spectrum was then recorded at room temperature. The amounts of BAS and LAS were calculated by a previously reported method²:

$$C_{BAS} = 1.88I_{A(B)}R^2/W$$

$$C_{LAS} = 1.42I_{A(L)}R^2/W$$

where $I_{A(B, L)}$ is the integrated absorbance of the BAS or LAS band, R is the radius of catalyst disk, W is the weight of disk.

NMR experiment

¹H, ²⁷Al and ²⁹Si MAS NMR and the 2D ²⁷Al-²⁹Si correlation NMR experiments were performed over an 11.7 T Bruker AVANCE-III spectrometer. The resonance frequencies were 500.6 MHz for ¹H, 130.4 MHz for ²⁷Al, 99.4 MHz for ²⁹Si. The ¹H and ²⁷Al MAS NMR and the 2D ²⁷Al-²⁹Si correlation NMR spectra were obtained by using a 4 mm triple-resonance probe at a spinning rate of 10 kHz. Hahn-echo pulse sequence ($\pi/2$ - τ - π - τ -acquisition) with a $\pi/2$ pulse width of 4.2 μ s and a repetition time of 2 s was used to record the ¹H MAS NMR spectra, where τ equals to one rotor period (100 μ s). Single-pulse sequence with a short pulse width of 0.20 μ s (ca. $\pi/12$ pulse) and a recycle delay of 1 s was used in the ²⁷Al MAS NMR experiments. For the two-dimension ²⁷Al-²⁹Si correlation NMR experiments, an initial WURST pulse was used on ²⁷Al channel with a length of 1 ms and an rf-field of $\nu_{27Al} = 2$ kHz. A π pulse of 20 μ s on ²⁷Al channel and two CT selective $\pi/2$ pulse of 7.5 μ s on ²⁹Si channel were used in the HMQC program.

Single-pulse ^{29}Si MAS NMR experiment with ^1H decoupling was performed on a 7mm double-resonance probe by using a $\pi/4$ pulse width of 3.2 μs and a repetition time of 60 s, the spinning rate was set to 5 kHz. The framework Si/Al ratio was calculated from the ^{29}Si MAS NMR spectra according to a classic procedure.³

$$Si/Al = \frac{\sum_{n=0}^4 I_{Si(nAl)}}{\sum_{n=0}^4 0.25nI_{Si(nAl)}}$$

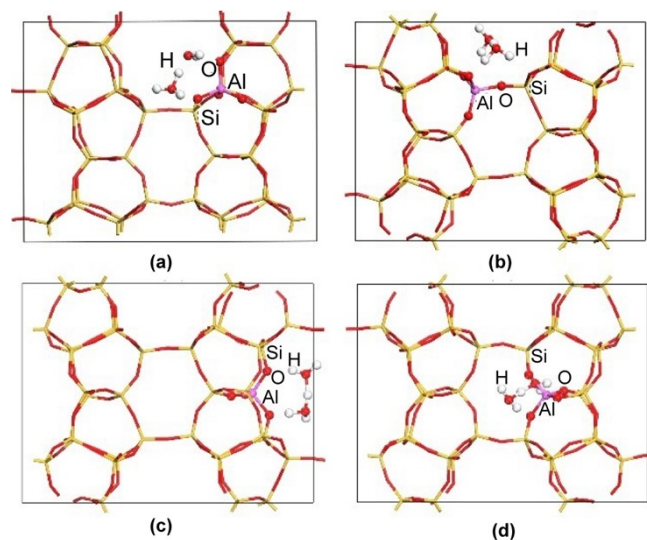
The 2D ^{27}Al triple-quantum (3Q) MAS z-filtering NMR experiment with fast amplitude modulation (FAM) enhancement was carried out on an 18.8 T Bruker AVANCE-III spectrometer using a 3.2 mm double-resonance probe with a spinning rate of 20 kHz. The resonance frequency of ^{27}Al was 208.6 MHz. The pulse duration was set to 4.8 μs for the first strong pulse with $\nu_{\text{RF}} \approx 125$ kHz. A FAM pulse train consists of 4 loops of two short pulses ($\nu_{\text{RF}} \approx 125$ kHz) and two delays with the same duration of 0.7 μs to convert $p = \pm 3$ to ± 1 coherences. The “soft” $\pi/2$ pulse was set to 10.4 μs . For comparison, the single-pulse ^{27}Al MAS NMR spectra at 18.8 T with a spinning rate of 20 kHz were collected by using a pulse width of 0.30 μs (ca. $\pi/12$ pulse) and a recycle delay of 1 s.

Adamantane at 1.91 ppm, 1 M $\text{Al}(\text{NO}_3)_3$ solution at 0 ppm and kaoline at -91.4 ppm were used as the references for calibrating the ^1H , ^{27}Al and ^{29}Si spectra, respectively. Analytical simulations of the NMR spectra were performed using the DMFIT program.

Computing methods

To assign the experimental NMR results, ^{27}Al chemical shifts at different T sites were calculated using the periodic boundary condition. The geometry optimizations were performed by using the DMol³ program^{4,5} with the generalized gradient approximation (GGA) proposed by Perdew-Burke-Ernzerhof (PBE) functional. The DND basis set and a default medium level Monkhorst-Pack K point ($1 \times 1 \times 2$) were adopted to sample the Brillouin zone. DFT-D method⁶ was used in structure optimization and NMR calculation to accurately describe the weak interaction in H-ZSM-35. During optimization, all the framework atoms and the adsorbed H_2O molecules were allowed to relax to their equilibrium positions. All of the ^{27}Al NMR shielding calculations were performed by the GIPAW method in the CASTEP-NMR code at the GGA/PBE level based on the optimized zeolite structures. Fine K point ($1 \times 1 \times 2$) and

cut-off energy of 550 eV were employed, combined with core-valance interactions described by ultrasoft pseudo potential generated on-the fly. The calculated ^{27}Al chemical shifts were further converted to ($\delta^{27}\text{Al}$) values, which were referred to the absolute shielding of Al at T1 site, namely 61 ppm for the experimental values.



Optimized structures of Al atom at T1 (a) T2 (b) T3 (c) and T4 (d) sites.

Catalytic tests

DME carbonylation was carried out on a continuous flow fixed-bed reactor (internal diameter, 8 mm). The catalyst (40-60 mesh, 300 mg) was loaded into the reactor and treated with N_2 (30 mL/min) at 773 K for 1 h. After cooling down to 493 K, a mixture of 5% DME/50% CO /2.5% N_2 /42.5% He was introduced through a mass-flow controller (6.25 mL/min) and the reactor was pressurized to 2.0 MPa. The effluent from the reactor was analyzed online using a gas chromatograph (Agilent 7890A) equipped with a 100% dimethylpolysiloxane column (HP-PONA, 50 m \times 0.20 mm \times 0.50 μm) that connected to a flame-ionization detector.

1-Butene isomerization was tested over the same equipment at ambient pressure. The catalyst (40-60 mesh, 100 mg) was loaded into the reactor and pre-treated with N_2 (30 mL/min) at 773 K for 1 h. After cooling down to 673 K under N_2 flow, the catalyst was exposed to a mixture of 10% 1-butene/2.5% Ar/He (50 mL/min). The effluent from the reactor was analyzed online using a gas chromatograph (Agilent 7890A) equipped with an Al_2O_3 column (HP-AL/M, 30 m \times 0.53 mm \times 15.0 μm) that connected to a flame-ionization detector.

Table S1. Texture properties of the FER zeolites

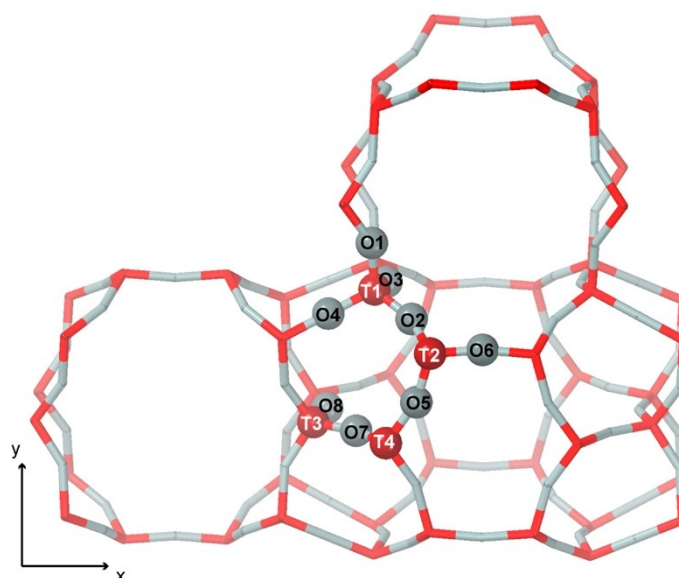
Sample	S_{BET} (m ² /g)	V_{total} (cm ³ /g)	V_{micro} (cm ³ /g)	V_{meso} (cm ³ /g)	S_{micro} (m ² /g)
ZSM-35-Diox	273.8	0.45	0.11	0.34	225.5
Zeolyst	251.8	0.27	0.10	0.17	207.1

Table S2. Acid properties of the FER zeolites

Sample	Si/Al ^a	Si/Al ^b	BAS (mmol/g) ^c	Al _{ex} ^d
ZSM-35-Diox	10.2	11.3	1.67	9.8%
Zeolyst	9.6	11.8	1.50	14.0%

^a Determined by ICP analysis; ^b Derived from the ²⁹Si MAS NMR spectra;

^c Estimated from the NH₃-TPD profile; ^d Estimated from the ²⁷Al MAS NMR spectra.



T-O-T	O location	T-O-T	O location
T1-O1-T3	10-MR	T2-O5-T4	6-MR
T1-O2-T2	8-MR window	T2-O6-T2	8-MR window, position to 10-MR
T1-O3-T1	8-MR window, position to 8-MR center	T3-O7-T4	FER cavity
T1-O4-T1	5-MR	T3-O8-T3	FER cavity

Scheme S1. Geometric locations of T sites (T1-T4) and oxygen atoms (O1-O8) in FER.

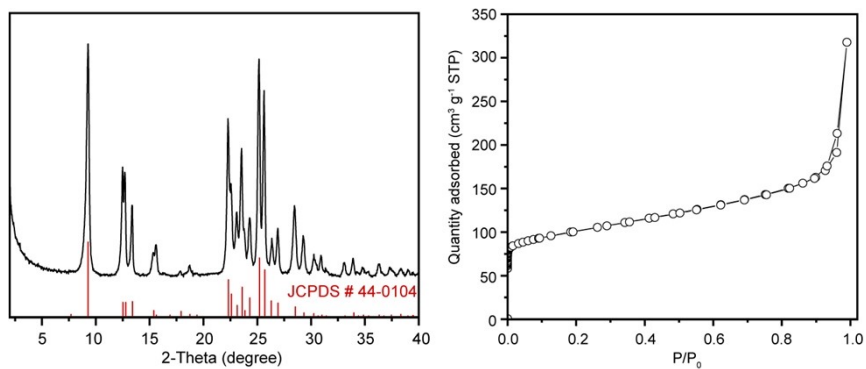


Figure S1. XRD pattern and N₂ adsorption isotherm of the ZSM-35-Diox sample.

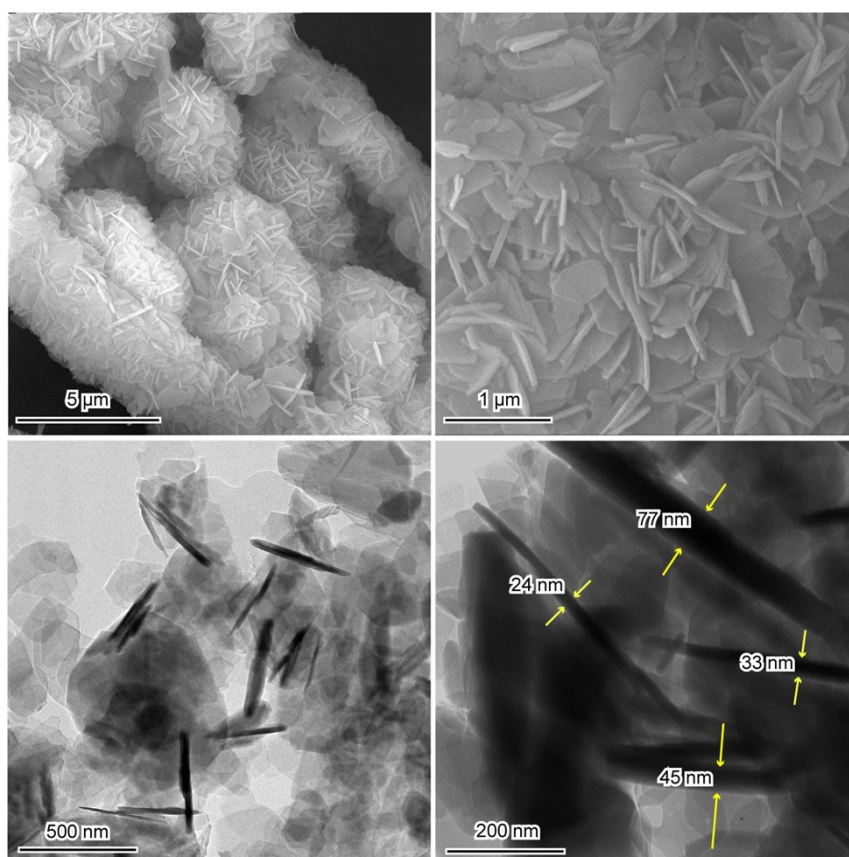


Figure S2. Additional SEM/TEM images of the ZSM-35-Diox sample.

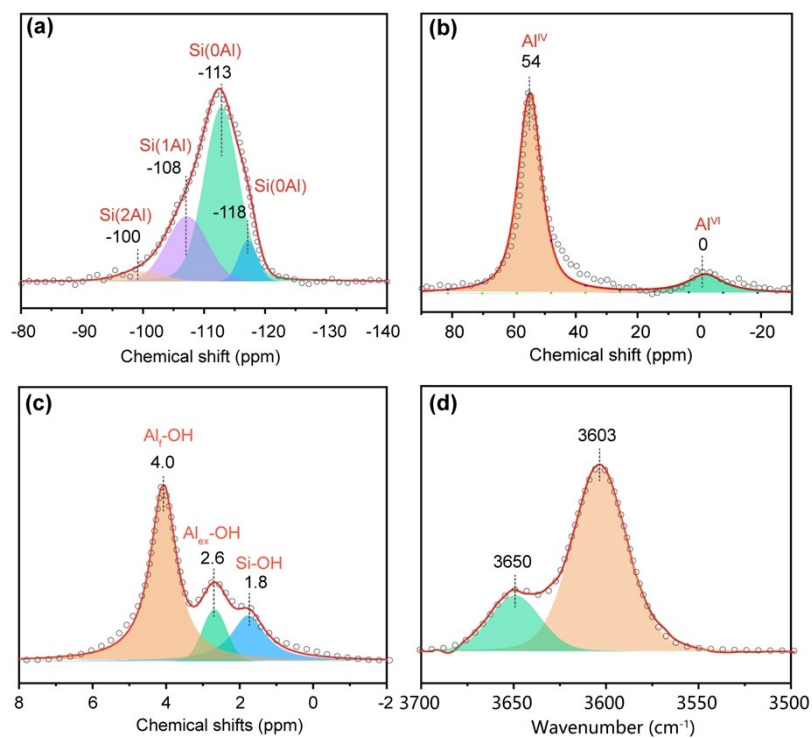


Figure S3. ^{29}Si , ^{27}Al , ^1H MAS NMR spectra (a-c) and IR spectrum (d) of the Zeolyst sample.

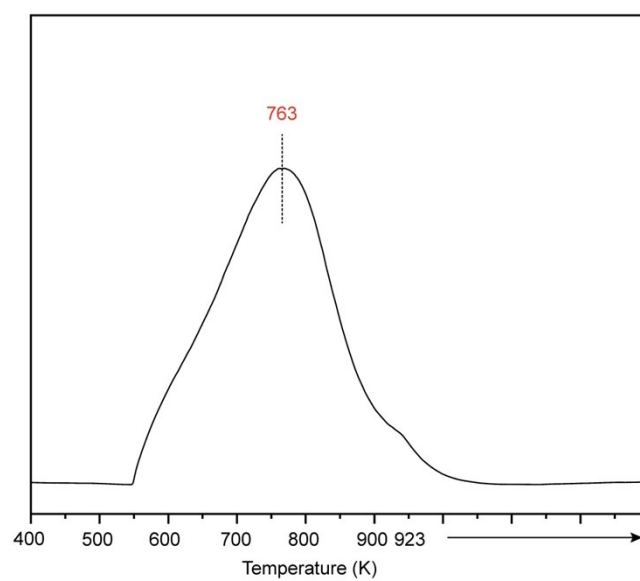


Figure S4. NH_3 -TPD profile of the ZSM-35-Diox sample.

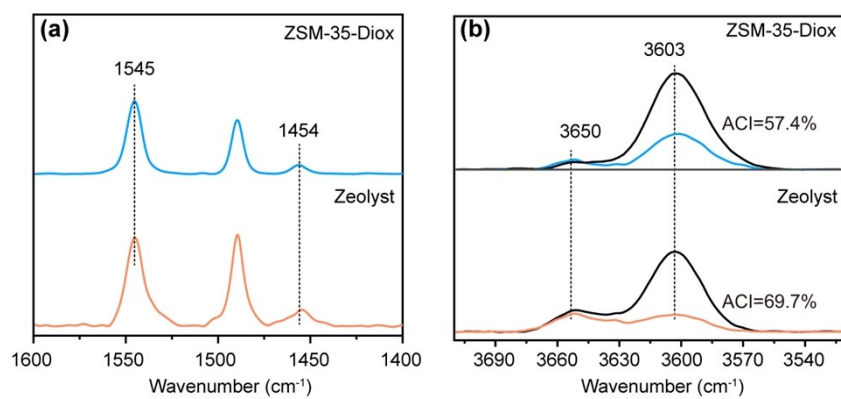


Figure S5. IR spectra of the FER zeolites at (a) 1600-1400 cm^{-1} after pyridine adsorption and (b) at 3603 cm^{-1} before and after pyridine adsorption.

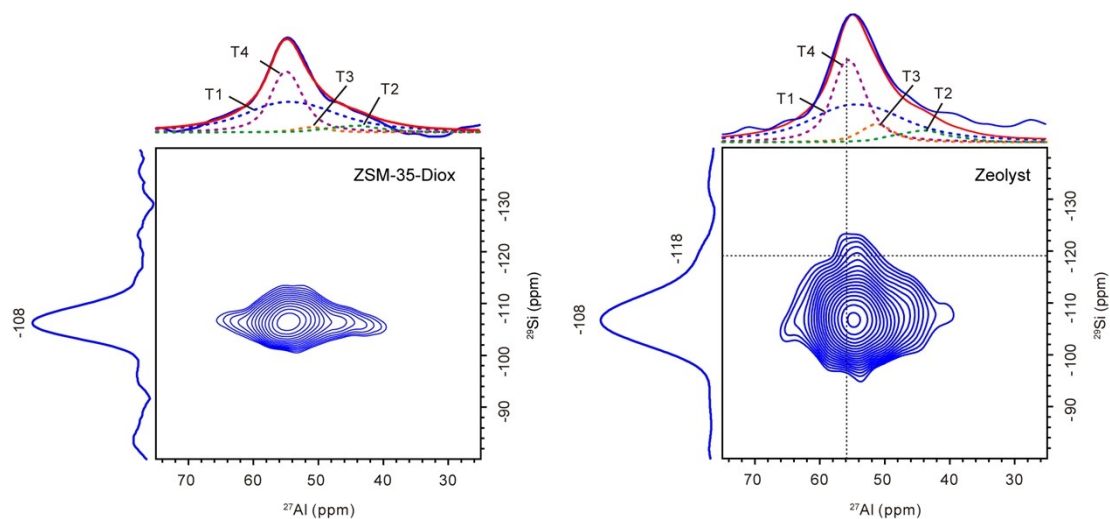


Figure S6. 2D $^{27}\text{Al}\{-^{29}\text{Si}\}$ D-HMQC MAS NMR spectra of the FER zeolites.

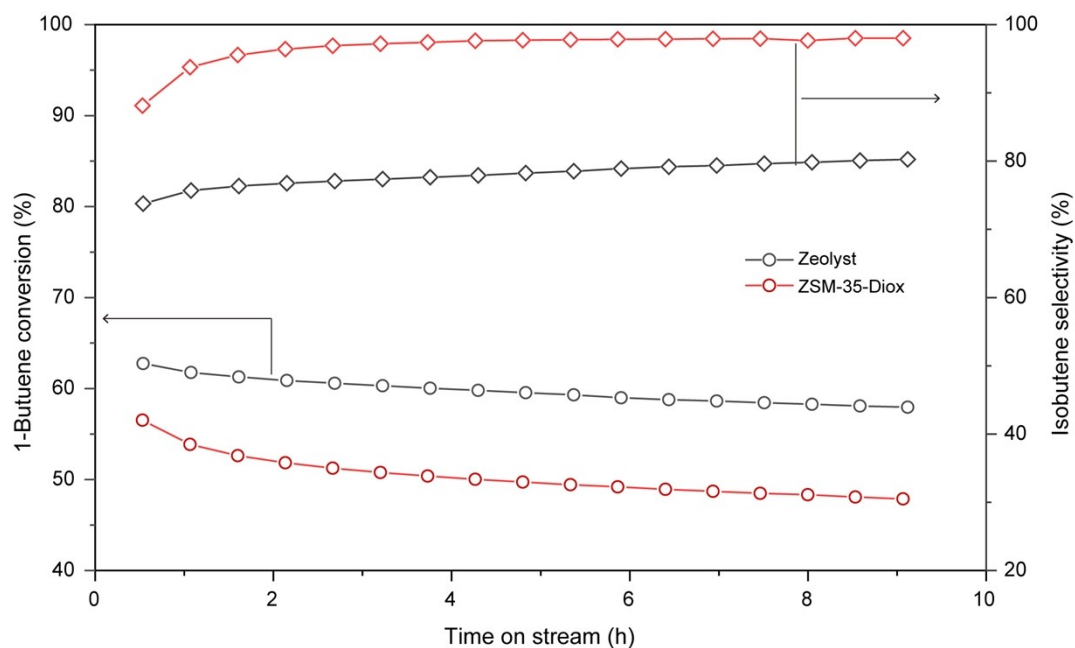


Figure S7. 1-Butene isomerization over the FER zeolites. Reaction conditions: 673 K, 10 vol% 1-C₄H₈/2.5 vol% Ar/He, 7.5 h⁻¹, ambient pressure.

References

- 1 G. Bagnasco, *J. Catal.*, 1996, **159**, 249-252.
- 2 C. A. Emeis, *J. Catal.*, 1993, **141**, 347-354.
- 3 J. Klinowski, S. Ramdas, J. M. Thomas, C. A. Fyfe and J. S. Hartman, *J. Chem. Soc., Faraday Trans.*, 1982, **78**, 1025-1050.
- 4 B. Delley, *J. Chem. Phys.*, 1990, **92**, 508-517.
- 5 B. Delley, *J. Chem. Phys.*, 2000, **113**, 7756-7764.
- 6 J. Chai and M. Head-Gordon, *Phys. Chem. Chem. Phys.*, 2008, **10**, 6615-6620.
- 7 Z. Xiong, E. Zhan, M. Li and W. Shen, *Chem. Commun.*, 2020, **56**, 3401-3404.